

## Quantifying grain size distribution of pedogenic magnetic particles in Chinese loess and its significance for pedogenesis

Qingsong Liu,<sup>1,2</sup> José Torrent,<sup>3</sup> Barbara A. Maher,<sup>4</sup> Yongjae Yu,<sup>5</sup> Chenglong Deng,<sup>2</sup> Rixiang Zhu,<sup>2</sup> and Xixi Zhao<sup>6</sup>

Received 8 March 2005; revised 10 June 2005; accepted 28 June 2005; published 18 November 2005.

[1] Quaternary glacial/interglacial cycles have been imprinted on the Chinese loess/paleosol sequences through pedogenesis. In order to accurately decode the paleoclimatic signals carried by these pedogenic particles it is essential to quantify the pedogenically produced magnetic particles in terms of mineralogy as well as grain size distribution (GSD). To date, the GSD has not been accurately determined because of the dearth of available means for analyzing extremely fine grained (nanometer-scale) pedogenic magnetic particles. Using low-temperature techniques, we systematically investigated the temperature dependency of  $\chi_{fd}$  (defined as  $\chi_{1\text{Hz}} - \chi_{10\text{Hz}}$ , where  $\chi_{1\text{Hz}}$  and  $\chi_{10\text{Hz}}$  are AC magnetic susceptibility measured at 1 and 10 Hz, respectively) from two characteristic loess profiles, one located at the western Chinese Loess Plateau and the other in the central plateau. On the basis of Néel theory for a shape anisotropy dominant grain and experimental analysis at low temperatures, a quantitative GSD for pedogenic particles in Chinese loess/paleosols was constructed. We found that the dominant magnetic grain size lies just above the superparamagnetic/single-domain threshold ( $\sim 20\text{--}25$  nm) and that the GSD is almost independent of the degree of pedogenesis. This observation agrees well with other constraints from previous studies. This new GSD model improves our understanding of the pedogenic processes in Chinese loess, enabling further explicit linkage of environmental magnetism to paleoclimate changes.

**Citation:** Liu, Q., J. Torrent, B. A. Maher, Y. Yu, C. Deng, R. Zhu, and X. Zhao (2005), Quantifying grain size distribution of pedogenic magnetic particles in Chinese loess and its significance for pedogenesis, *J. Geophys. Res.*, *110*, B11102, doi:10.1029/2005JB003726.

### 1. Introduction

[2] Since the beginning of the systematic studies on loess in the early 1980s, environmental magnetism has played an irreplaceable role in quantifying the paleoclimatic signals recorded by these high-resolution Quaternary sequences. Environmental magnetic techniques are not only fast and nondestructive, but they can also sensitively determine the physical properties of magnetic assemblage in terms of

grain size and mineralogy, which in turn sensitively reflects changes in paleoenvironment.

[3] For the past two decades the basic paleoenvironmental significance of magnetic proxies has been well exploited. For example, the Chinese loesses, interbedded by paleosols, record paleoclimate fluctuations [e.g., *Heller and Liu*, 1986; *Kukla et al.*, 1988; *Maher and Thompson*, 1991, 1992, 1995; *An and Porter*, 1997; *Porter*, 2001; *Ding et al.*, 2002]. A direct correlation of paleoclimatic signals between Chinese loess/paleosols and marine sediments reveals a global-scale paleoclimatic variation [*Heller and Liu*, 1984, 1986; *Kukla et al.*, 1988, 1990; *Hovan et al.*, 1989; *Thompson and Maher*, 1995; *Ding et al.*, 2002]. Reviews of loess magnetism and its paleoenvironmental applications were given by *Heller and Evans* [1995], *Maher and Thompson* [1999], *Porter* [2001], and *Tang et al.* [2003]. The magnetic enhancement of the Chinese loess has been attributed to the formation of fine-grained ferrite particles through pedogenic processes [e.g., *Zhou et al.*, 1990]. Traditionally, the fine-grained pedogenic particles for magnetic enhancements have been interpreted as maghemite [*Verosub et al.*, 1993; *Sun et al.*, 1995]. However, we cannot exclude the possibility that their initial mineral phase is magnetite [*Maher and Thompson*, 1995], which is subse-

<sup>1</sup>Now at Institute for Rock Magnetism and Department of Geology and Geophysics, University of Minnesota, Minneapolis, Minnesota, USA.

<sup>2</sup>Paleomagnetism and Geochronology Laboratory (SKL-LE), Institute of Geology and Geophysics, Chinese Academy of Sciences, Beijing, China.

<sup>3</sup>Departamento de Ciencias y Recursos Agrícolas y Forestales, Universidad de Córdoba, Córdoba, Spain.

<sup>4</sup>Centre for Environmental Magnetism and Palaeomagnetism, Lancaster Environment Centre, Geography Department, Lancaster University, Lancaster, UK.

<sup>5</sup>Geosciences Research Division, Scripps Institution of Oceanography, La Jolla, California, USA.

<sup>6</sup>Department of Earth Sciences, University of California, Santa Cruz, California, USA.

quently oxidized into maghemite. *Maher et al.* [2003] show that the magnetic data from the modern soils of both the Chinese Loess Plateau and the loessic Russian steppe are highly correlated. Because pedogenesis is controlled by several factors, including parent material, climate, biological organisms, topography, and time, such a correlation of magnetic data between two well-isolated regions suggests that only one or a few of them is dominant. The most likely factor is the amount of precipitation [*Maher et al.*, 2003].

[4] In the past, the grain size distribution (GSD) of pedogenic particles in loess has been confined within the superparamagnetic (SP) and single-domain (SD) grain size range [*Zhou et al.*, 1990; *Maher and Thompson*, 1991, 1992, 1995; *Hunt et al.*, 1995]. However, the exact quantitative distribution of these particles has not been clearly demonstrated.

[5] On the basis of the Néel theory [*Néel*, 1949], *Liu* [2004] recently developed a new low-temperature technique using the temperature dependence of  $\chi_{fd}$  (defined as  $\chi_{1\text{Hz}} - \chi_{10\text{Hz}}$ , where  $\chi_{1\text{Hz}}$  and  $\chi_{10\text{Hz}}$  are AC magnetic susceptibility measured at 1 and 10 Hz, respectively). This technique is extremely powerful in recognizing the existence of fine-grained ferrimagnetic particles [*Liu*, 2004]. In this study, we intend to precisely determine the GSD of fine-grained pedogenic particles in Chinese loess from the temperature dependence of  $\chi_{fd}$ . The paleoclimatic significance of this new GSD model will also be discussed.

## 2. Samples and Experimental Procedure

[6] Two sets of samples were selected from the Yuanbao (YB, 35°38'N/103°10'E) and Yichuan (YC, 36°03'N/110°10'E) loess/soil profiles. We note that the maximum susceptibility at YC is about twice as high as that at YB, indicating a greater degree of pedogenesis at YC. Three samples, at depths of 38.94 (YB1), 39.04 (YB2), and 39.24 m (YB3), at YB were selected from the subpaleosol unit S1S3 (marine oxygen isotope stage, MIS5e) (Figure 1a). YB is located in the northwestern margin of the Chinese Loess Plateau, on the fourth terrace of the Daxia River in the Linxia Basin. To remove any possible contribution of aeolian, coarse-grained magnetite particles to the measured low-temperature properties, these particles were magnetically extracted using a continuous loop flow driven by a pump with a high-gradient magnet [*Hounslow and Maher*, 1996].

[7] The YC loess section is located ~300 km northeast of Xian. Three samples were selected from the paleosol unit S1 at depths of 8.80 (YC1), 8.95 (YC2), and 10.40 m (YC3) (Figure 1d). The combined frequency (1 and 10 Hz in fields of ~240 A/m, or 0.3 mT) and low-temperature dependence (10–300 K) of susceptibility (hereinafter refer to  $\chi_{fd} - T$ , where  $\chi_{fd} = \chi_{1\text{Hz}} - \chi_{10\text{Hz}}$  and  $T$  represents temperature) was measured using a Quantum Design superconducting quantum interference device (SQUID) Magnetic Properties Measurement System (MPMS).

[8] We picked six representative samples from the two independent loess profiles on the following grounds. First, the rock magnetic properties of these two profiles have been well examined by previous studies [*Liu*, 2004]. Second, previous analysis shows a narrow GSD for these samples. For example, the  $\chi_{fd}\%$  value (defined as  $(\chi_{470\text{Hz}} -$

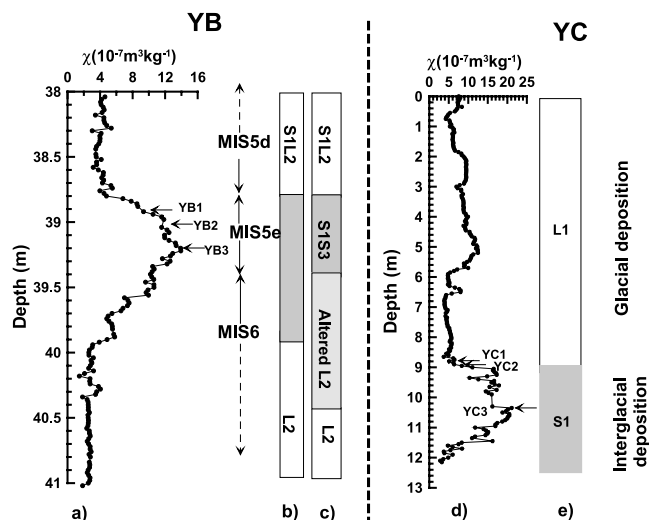


**Figure 1.** Depth profiles of magnetic susceptibility (a) for YB and (d) for YC and the corresponding pedostratigraphy (b and c) for YB and (e) for YC. Arrows indicate sampling locations [after *Chen et al.*, 1999; *Liu et al.*, 2004c].

$\chi_{470\text{Hz}})/\chi_{470\text{Hz}}$ ) of YB is ~14% after removing the contributions from aeolian inputs, suggesting that pedogenic particles in the Chinese paleosols have a uniform GSD [*Liu et al.*, 2004a]. In other words, variations in magnetic susceptibility are dominantly controlled by varying concentrations of pedogenic magnetite/maghemite particles, and the changes in magnetic properties between two end-members (loess and mature paleosol defined by the lowest and highest magnetic susceptibility, respectively) are predictable. Third, despite their similar ages all three samples of YB and MIS5e of YC are from two localities with substantially different rainfall regimes. In contrast, YC1 and YC2 of YC are from MIS5a. Therefore samples from different ages can be compared within a single site at YC.

[9] The Chinese loess/paleosol sequence consists of periodically alternating less altered loess horizons and highly weathered paleosol layers, which were deposited during cold/arid and warm/humid climate, respectively. A dominant magnetic phase in the aeolian loess is coarse-grained (pseudosingle domain, PSD; multidomain, MD), partially oxidized magnetite [*Liu*, 2004]. Note that loess samples were not analyzed because they do not contain significant amount of SP + SD magnetic particles.

## 3. Results

[10] All samples from the two distinct sites exhibit a consistent low-temperature pattern. With increasing frequency from 1 to 10 Hz,  $\chi$  decreases (Figure 2). For  $T < \sim 40$  K,  $\chi$  gradually decreases with increasing temperature, indicating that paramagnetic components are dominant. Above 40 K,  $\chi$  increases with further increases in temperature, mainly due to the unblocking of SP particles [e.g., *Liu*, 2004]. For the YB samples (Figures 2a–2c), because the coarse-grained aeolian magnetites have been extracted, no Verwey transition (at ~120 K) was detected. In contrast, for the intermediate paleosols (Figures 2e and 2f) a slight deflection at ~120 K indicates the presence of magnetite.

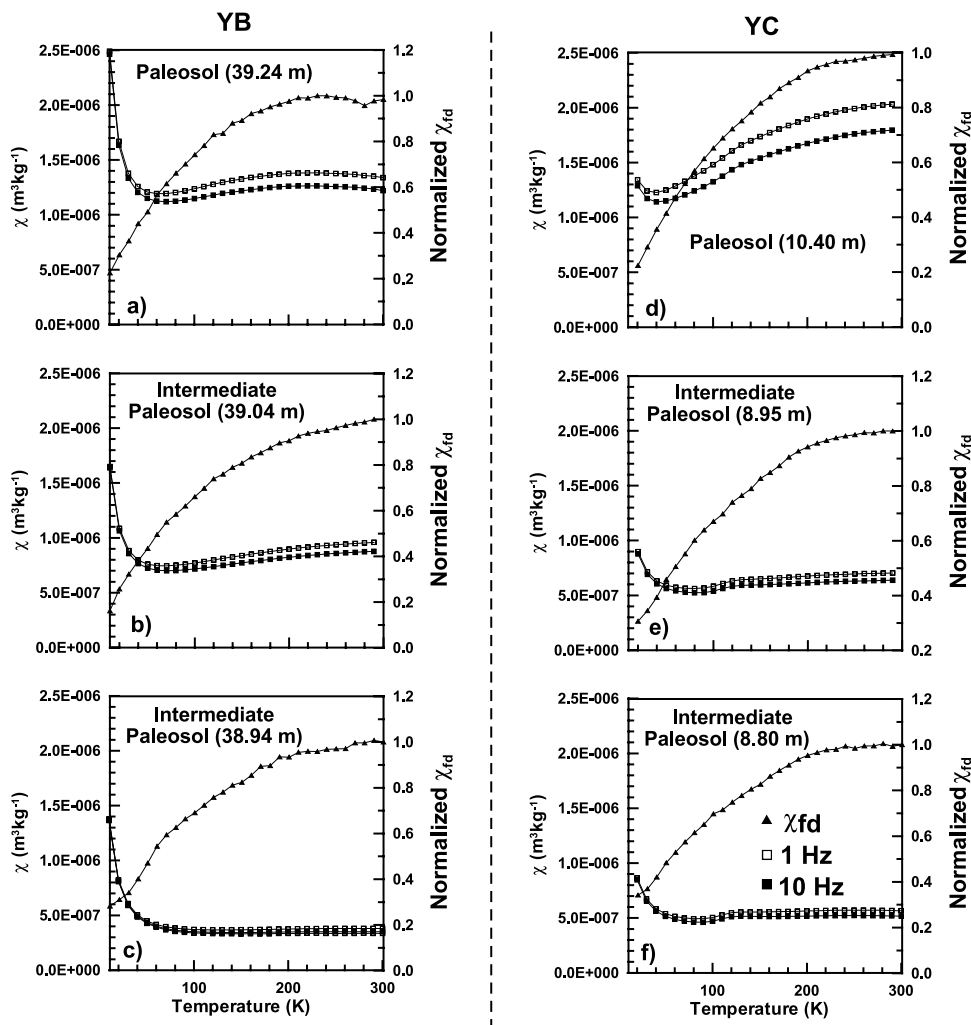


**Figure 2.** Temperature dependency of magnetic susceptibility ( $\chi_{1\text{Hz}}$ , open rectangle;  $\chi_{10\text{Hz}}$ , solid rectangle; and  $\chi_{1\text{Hz}} - \chi_{10\text{Hz}}$ , solid triangle).

However, it is apparent that the aeolian components do not contribute to  $\chi_{fd}$  (Figures 2e and 2f) because they are equally influencing susceptibility measured at 1 and 10 Hz.

#### 4. On the Use of $\chi_{fd} - T$ for Granulometry

[11] On the basis of the Néel theory, *Worm* [1998] systematically investigated the frequency dependence of superparamagnetic particles. Assuming temperature-independent saturation magnetization ( $M_s$ ) and macroscopic coercivity ( $H_k$ ) at  $<300$  K, *Jackson and Worm* [2001] simulated the in-phase and quadrature components of susceptibility. Most recently, *Liu* [2004] incorporated the temperature dependence both for  $M_s$  and  $H_k$  and developed new approaches to quantify the GSD for fine-grained ferrimagnetic particles.

[12] Fine-grained ferrimagnetic particles ( $<\sim 100$  nm) change their magnetic properties sharply with increasing grain sizes. Around  $\sim 20\text{--}25$  nm, just smaller than the blocking volume, their susceptibilities are highly frequency-dependent (so called viscous superparamagnetic (VSP)). Above the VSP threshold, magnetic particles become blocked in stable SD states, and therefore their susceptibilities

are frequency-independent. Below the VSP threshold the susceptibilities of these particles are independent of frequency because their relaxation time is less than the time constants for the susceptibility measurements; their behavior is truly SP. As a result, when we compare susceptibilities measured at two different frequencies, the difference ( $\chi_{fd}$ ) occurs only for the VSP grains. In addition, the grain size displaying the maximum of  $\chi_{fd}$  (named  $D_{\chi_{fd}\text{-max}}$ ) is strongly temperature-dependent. With decreasing temperature,  $D_{\chi_{fd}\text{-max}}$  gradually shifts to finer grain sizes (Figure 3). Therefore the temperature domain can be translated into a magnetic grain size proxy [*Liu*, 2004] (Figure 4).

[13] In our model we assume that  $H_k$  is controlled by shape anisotropy as in the study by *Jackson and Worm* [2001]. A dominant shape anisotropy in magnetism is commonly observed in natural rocks [e.g., *Thompson and Oldfield*, 1986] and synthetic iron oxides [e.g., *Yu et al.*, 2002]. Note that the grain size is insensitive to slight changes in coercivity. For example, an increase of coercivity by  $\sim 10\%$  from 22.5 to 25 mT induces a corresponding change in the diameter only for  $\sim 3\%$ .

[14] The correlation between  $T$  and  $D_{\chi_{fd}\text{-max}}$  is shown in Figure 4. The temperature dependence of  $\chi_{fd}$  for the six

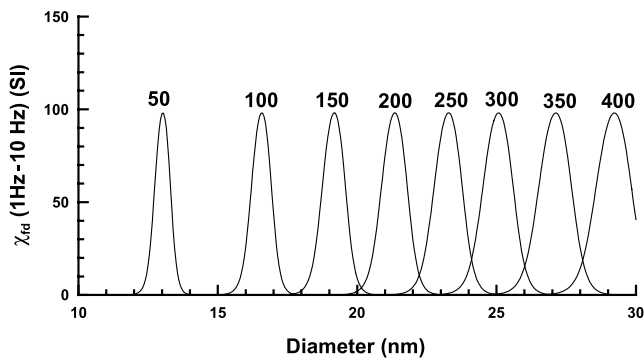


**Figure 3.** Predicted correlation between grain size and temperature dependence of magnetic susceptibility for maghemite, which is controlled by shape anisotropy.  $D_{\chi_{fd}-\max}$  is a position where the maximum temperature dependence of magnetic susceptibility was observed. We used a room temperature coercivity of 22.5 mT in calculation.

representative samples is illustrated in Figure 5a. Overall, all samples show consistent patterns that  $\chi_{fd}$  increased with increasing temperature and gradually saturated above  $\sim 220$  K. A normalized  $\chi_{fd} \sim D_{\chi_{fd}-\max}$  represents the GSD of fine-grained pedogenic particles (Figure 5b). It is apparent that the GSD is almost independent of the degree of pedogenesis. For comparison, we inserted an average curve for the measured six samples (Figure 5b).

[15] In Figures 3 and 4, average grain size can be inferred from the position of peak temperature. Strictly speaking, we need to consider a blocking process statistically associated with uncertainty estimation because blocking occurs over a period of time and temperature interval. Fortunately, Figure 3 provides a practical solution with a reasonable indication of uncertainty in the model. For example, each peak has a width of 1 nm or so, although peaks show a tendency to be narrower as temperature decreases. A much more rigorous approach involving deconvolution of raw data is necessary only when the inherent blurring in the measurements obscures sharp variations, as in u-channel paleomagnetic records. Instead, it may be fair to assume a smooth variation of GSD in most natural samples.

[16] The GSD for fine-grained magnetic particles in soils is often continuous and has been generally fitted by a lognormal volume distribution [Eyre, 1997; Worm, 1998]. Here a lognormal volume distribution was fitted to the average GSD obtained between about 10 and 25 nm and then extrapolated to  $\sim 100$  nm (Figure 6).

## 5. Discussion

### 5.1. Grain Size Distribution Model

[17] Maher's [1988] work on the magnetic properties of submicron magnetite particles made it feasible to detect these ultrafine magnetic particles in the Chinese loess. Zhou *et al.* [1990] proposed that the magnetic enhancement of the Chinese loess was partially due to the in situ formation of fine-grained (e.g., superparamagnetic (SP)) pedogenic particles, which is supported by Maher and Thompson [1991] as well. SD particles play a key role in controlling the magnetic enhancement, rather than SP particles, because

they have a much higher volume fraction than the latter, although both of them covary with the degree of pedogenesis [Eyre and Shaw, 1994; Florindo *et al.*, 1999; Deng *et al.*, 2004; Liu, 2004].

[18] The second important feature of pedogenic magnetic particles is that they have low coercivities. Heller and Evans [1995], for example, documented that samples from Baicaoyuan in the arid western Chinese Loess Plateau decrease their coercivity from 18.4 mT for the least pedogenically altered loesses sharply down to 8.5 mT for the paleosols. Such a decrease in coercivity due to pedogenesis is generally observed in the Loess Plateau region, from western to eastern or to southern plateau [Evans and Heller, 1994, 2001; Fukuma and Torii, 1998; Maher and Thompson, 1999; Deng *et al.*, 2005].

[19] The relatively high coercivity of less weathered loess samples is not of SD origin; rather it is caused by low-temperature oxidation of the coarse-grained (PSD and MD) aeolian magnetic particles [van Velzen and Dekkers, 1999]. In contrast, the low coercivity of the magnetic particles in paleosols indicates that the newly formed pedogenic particles are not in stable SD grain size region, but are probably located just above the SP/SD threshold ( $\sim 20$ – $25$  nm [Maher and Thompson, 1992, 1999]). Moreover, they have been completely oxidized into maghemite. Our new results (Figure 5b) show that the dominant grain sizes of pedogenic particles are indeed just above the SP/SD threshold.

[20] The third feature of the pedogenic magnetic particles is that they have a fairly consistent GSD, as shown in the present study. It is also interesting that this constant GSD appears to be independent of the degree of pedogenesis (Figure 5). This can be further supported by studies of Forster *et al.* [1994], Forster and Heller [1997], Maher *et al.* [2003], and Liu *et al.* [2004a]. The degree of observed magnetic enhancement is thus dominantly determined by changes in the concentration of the pedogenic particles. Hence a two-component model can adequately explain the enhancement pathways of magnetic properties of the Chinese loess [Forster and Heller, 1997; Mishima *et al.*, 2001]. In addition, soil development in the Chinese loess can be described as a consistent model [Liu *et al.*, 2004c], indicat-

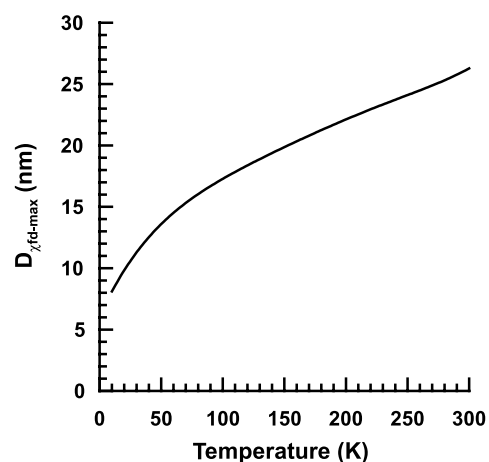


**Figure 4.** Correlation between  $D_{\chi_{fd}-\max}$  and temperature for maghemite. The room temperature  $B_c$  is set to 22.5 mT without considering thermal fluctuations.



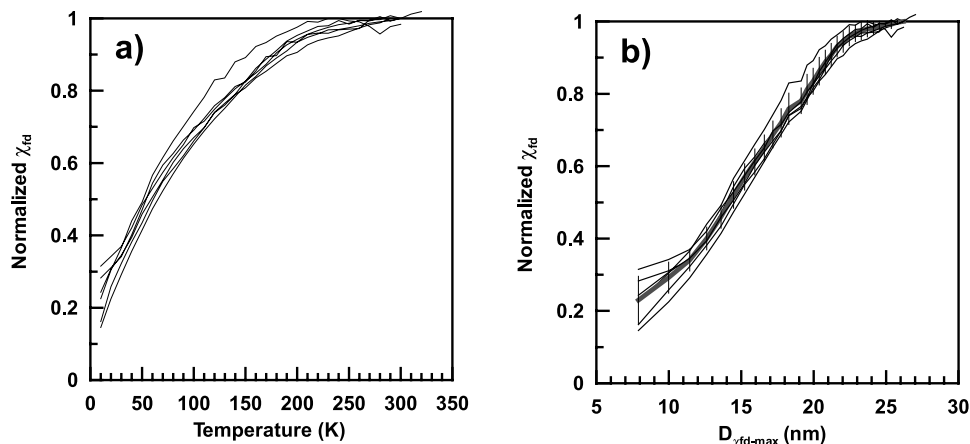


**Figure 5.** (a) Temperature dependence of  $\chi_{fd}$  and (b) grain size distribution of pedogenic particles in samples from YB and YC. The shaded curve with error bars in Figure 5b represents a mean trend.

ing that the magnetic signals across the Loess Plateau are directly comparable. Conversely, different enhancement pathways have been reported previously [e.g., *Maher and Thompson, 1999; Forster and Heller, 1997*]. In their models, *Forster and Heller [1997]* recognized different degrees of magnetic “hardness” or “softness” from four different regions of the Loess Plateau, depending on the relative amounts of the original aeolian mixture and pedogenic fine-grained magnetic particles. Therefore the seemingly different pathways could be mainly due to differences in the aeolian inputs and are independent of the in situ pedogenesis. A slightly different magnetic enhancement pathway could also be due to other climate variables (e.g., seasonality) besides the amount of precipitation [*Maher et al., 2003*].

[21] In summary, the GSD of pedogenic magnetic particles in the Chinese loess is concentrated in the nanometer range with a dominant grain size located just above the SP/

SD threshold ( $\sim 20\text{--}25$  nm [*Maher and Thompson, 1991, 1992, 1995*]). The volume contribution of SD particles is much higher than that of SP particles [*Liu et al., 2004b*]. In addition, this distribution is almost independent of pedogenesis.

[22] Our approach relies on the assumption that shape anisotropy is dominant for the pedogenic maghemite particles. In Figure 6, GSD estimation is generally well matched with a lognormal volume distribution, but there exists slight deviation at smaller volumes. It is possible that magnetocrystalline contribution [e.g., *Yu et al., 2004*] may cause such a tiny discrepancy.

[23] Regardless of whether shape or magnetocrystalline anisotropy controls magnetic properties of a pedogenic particle, our approach yields the same trend as in Figure 6, indicating a uniform GSD. For instance, prior to the transformation from a temperature domain to a grain size domain (Figure 4) the six representative samples have

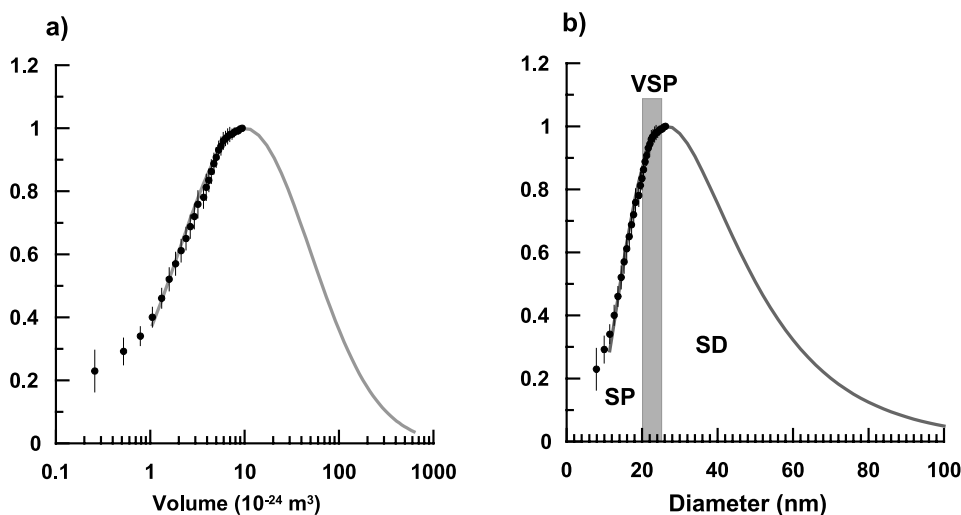


**Figure 6.** (a) Normalized volume distribution and (b) grain size distribution of pedogenic particles in the Chinese loess. The shaded curves represent a best fitting lognormal distribution fitting to data above  $1 \times 10^{-24} \text{ m}^3$  because data smaller than that may have been controlled by magnetocrystalline anisotropy rather than shape anisotropy. The thick shaded bar in Figure 6b represents a range of grain size for VSP. Note that the equivalent diameter is calculated by assuming a spherical maghemite grain.

fairly consistent and continuous grain size distributions (Figure 5a). It is worth noting that  $\chi_{fd}\%$  alone falls short of faithfully reflecting the GSD because it is sensitive only to a very narrow portion of the GSD near the SP/SD threshold.

## 5.2. Pedogenic Significance

[24] Possible origins for fine-grained magnetic particles include (1) intracellular magnetite production via bacteria, (2) extracellular formation of magnetite mediated by the action of iron-reducing bacteria, and (3) inorganic iron redox processes during pedogenesis. Intracellular magnetite crystals (magnetosomes) have species-specific crystal morphology, and they usually show a narrow grain size distribution within the SD grain size region [e.g., *Bazylinski et al.*, 1988; *Hanzlik et al.*, 1996]. Hence this mechanism is unlikely to explain the presence of much finer SP grains within Chinese paleosols. Postformation dissolution of bacterially produced SD grains could result in smaller grains, but it cannot produce a fixed GSD, as observed in this study. During pedogenesis in the loess/paleosols, organic matter and iron-reducing bacteria may play a key role in producing a local reducing environment [*Maher and Thompson*, 1995]. Under this reducing environment, hematite or other iron (III) oxides can be reduced to magnetite [*Maher*, 1998] and subsequently oxidized into maghemite. Maghemite in soils can be formed through various processes: (1) heating of goethite in the presence of organic matter [*Schwertmann*, 1989], (2) partial oxidation of magnetite, (3) dehydration of lepidocrocite, (4) from precursor ferrihydrite [*Barrón and Torrent*, 2002; *Barrón et al.*, 2003], and (5) reduction of hematite to magnetite and subsequent oxidation to maghemite.

[25] A conceptual model is that iron is released by weathering from primary Fe-bearing minerals by oxidation at mineral surfaces. The  $\text{Fe}^{2+}$  ions produced may be incorporated as  $\text{Fe}^{3+}$  or  $\text{Fe}^{2+}$  into an iron oxide phase in situ [*Maher*, 1998]. The most common and the first alteration products of aeolian Fe-bearing silicates are hematite ( $\alpha\text{Fe}_2\text{O}_3$ ), goethite ( $\alpha\text{FeOOH}$ ), and/or ferrihydrite. *Schwertmann* [1989] has shown that pedogenic alteration of Fe-bearing silicates leads to the production of goethite and hematite in humid and arid climates, respectively. Subsequently, these iron (III) oxides could be reduced to magnetite.

[26] If this conceptual model is valid, a constant GSD requires that the magnetite formation must be initialized under "constant" environmental conditions. One possible mechanism is that the  $\text{Fe}^{2+}$ -produced bacteria in the natural environment are active only within a certain set of pH, Eh, and Fe conditions [*Maher et al.*, 2003]. For example, *Taylor et al.* [1987] experimentally showed that the special GSD for the Chinese soils could be produced with a pH of 7.5, a mean temperature of 26°C, and an oxidation rate of 4 mL/min. Another possible mechanism for maghemite formation is directly from ferrihydrite [*Barrón and Torrent*, 2002; *Barrón et al.*, 2003]. In this model, maghemite particles produced in this way lie mostly within the 20–40 nm size range, and particle size does not depend on the temperature of formation. Particles gradually grow from several nanometers up to the SD grain size region with time. If this model is applicable to the Chinese loess, the grain sizes of the pedogenic

particles can quickly reach their equilibrium state, then the GSD of pedogenic maghemite should remain the same regardless of the degree of pedogenesis and the environmental conditions (temperature, hydrological regime) in which the paleosols formed. This model predicts hematite rather than goethite as a dominant antiferromagnetic phase.

## 6. Conclusions

[27] Our main conclusion is that pedogenesis produces a similar GSD at different localities with different conditions during MIS5. Assuming that the pedogenic magnetic particles are controlled by shape anisotropy, a dominant grain size maximum is estimated to be just above the SP/SD threshold ( $\sim 20\text{--}25$  nm) but can be extended to the upper boundary of the SD particles at  $\sim 100$  nm on the basis of the lognormal volume distribution model. This new GSD model provides new insights into the mechanisms for the formation of the fine-grained magnetic particles through pedogenesis in the Chinese Loess Plateau.

[28] **Acknowledgments.** We are grateful to B. Carter-Stiglitz and F. H. Chen for providing samples. We also thank two anonymous reviewers, the Associate Editor, and Subir Banerjee and Mike Jackson for their helpful suggestions. This study is supported by the National Natural Science Foundation of China grants 40221402 and 40325011, the Spanish Ministerio de Ciencia y Tecnología, Project AGL2003–01510, and by the U.S. National Science Foundation grant OCE 0327431. All rock magnetic measurements were made at the IRM, which is supported by the W. M. Keck Foundation, the Earth Science Division of the U.S. National Science Foundation, and the University of Minnesota. This is IRM publication 0505.

## References

- An, Z. S., and S. C. Porter (1997), Millennial-scale climatic oscillations during the last interglaciation in central China, *Geology*, *25*, 603–606.
- Barrón, V., and J. Torrent (2002), Evidence for a simple pathway to maghemite in Earth and Mars soils, *Geochim. Cosmochim. Acta*, *66*, 2801–2806.
- Barrón, V., J. Torrent, and E. De Grave (2003), Hydromaghemite, an intermediate in the hydrothermal transformation of 2-line ferrihydrite into hematite, *Am. Mineral.*, *88*, 1679–1688.
- Bazylinski, D. A., R. B. Frankel, and H. W. Jannasch (1988), Anaerobic magnetite production by a marine, magnetotactic bacterium, *Nature*, *334*, 518–519.
- Chen, F. H., J. Bloemendal, Z. D. Feng, J. M. Wang, E. Parker, and Z. T. Guo (1999), East Asian monsoon variations during oxygen isotope stage 5: Evidence from the northwestern margin of the Chinese Loess Plateau, *Quat. Sci. Rev.*, *18*, 1127–1135.
- Deng, C., R. Zhu, K. L. Verosub, M. J. Singer, and N. J. Vidic (2004), Mineral magnetic properties of loess/paleosol couplets of the central Loess Plateau of China over the last 1.2 Myr, *J. Geophys. Res.*, *109*, B01103, doi:10.1029/2003JB002532.
- Deng, C., N. J. Vidic, K. L. Verosub, M. J. Singer, Q. Liu, J. Shaw, and R. Zhu (2005), Mineral magnetic variation of the Jiaodao Chinese loess/paleosol sequence and its bearing on long-term climatic variability, *J. Geophys. Res.*, *110*, B03103, doi:10.1029/2004JB003451.
- Ding, Z. L., E. Derbyshire, S. L. Yang, Z. W. Yu, S. F. Xiong, and T. S. Liu (2002), Stacked 2.6-Ma grain size record from the Chinese loess based on five sections and correlation with the deep-sea  $\delta^{18}\text{O}$  record, *Paleoceanography*, *17*(3), 1033, doi:10.1029/2001PA000725.
- Evans, M. E., and F. Heller (1994), Magnetic enhancement and palaeoclimate: A study of a loess/paleosol couplet across the Loess Plateau of China, *Geophys. J. Int.*, *117*, 257–264.
- Evans, M. E., and F. Heller (2001), Magnetism of loess/paleosol sequences: Recent developments, *Earth Sci. Rev.*, *54*, 129–144.
- Eyre, J. K. (1997), Frequency dependency of magnetic susceptibility for populations of single-domain grains, *Geophys. J. Int.*, *129*, 209–211.
- Eyre, J. K., and J. Shaw (1994), Magnetic enhancement of Chinese loess—The role of  $\gamma\text{Fe}_2\text{O}_3$ ?, *Geophys. J. Int.*, *117*, 265–271.
- Florindo, F., R. Zhu, B. Guo, L. Yue, Y. Pan, and F. Speranza (1999), Magnetic proxy climate results from the Duanjiapo loess section, south-

- ernmost extremity of the Chinese Loess Plateau, *J. Geophys. Res.*, *104*, 645–659.
- Forster, T., and F. Heller (1997), Magnetic enhancement paths in loess sediments from Tajikistan, China, and Hungary, *Geophys. Res. Lett.*, *24*, 17–20.
- Forster, T., M. E. Evans, and F. Heller (1994), The frequency dependence of low field susceptibility in loess sediments, *Geophys. J. Int.*, *118*, 636–642.
- Fukuma, K., and M. Torii (1998), Variable shape of magnetic hysteresis loops in the Chinese loess-paleosol sequence, *Earth Planets Space*, *50*, 9–14.
- Hanzlik, M., M. Winklhofer, and N. Petersen (1996), Spatial arrangement of chains of magnetosomes in magnetotactic bacteria, *Earth Planet. Sci. Lett.*, *145*, 125–134.
- Heller, F., and M. E. Evans (1995), Loess magnetism, *Rev. Geophys.*, *33*, 211–240.
- Heller, F., and T. S. Liu (1984), Magnetism of Chinese loess deposits, *Geophys. J. R. Astron. Soc.*, *77*, 125–141.
- Heller, F., and T. S. Liu (1986), Palaeoclimatic and sedimentary history from magnetic susceptibility of loess in China, *Geophys. Res. Lett.*, *13*, 1169–1172.
- Hounslow, M. W., and B. A. Maher (1996), Quantitative extraction and analysis of carriers of magnetization in sediments, *Geophys. J. Int.*, *124*, 57–74.
- Hovan, S. A., D. K. Rea, N. G. Pisias, and N. J. Shackleton (1989), A direct link between the China loess and marine  $\delta^{18}\text{O}$  records: Aeolian flux to the North Pacific, *Nature*, *340*, 296–298.
- Hunt, C. P., S. K. Banerjee, J. M. Han, P. A. Solheid, E. Oches, W. W. Sun, and T. S. Liu (1995), Rock-magnetic proxies of climate change in the loess-paleosol sequences of the western Loess Plateau of China, *Geophys. J. Int.*, *123*, 232–244.
- Jackson, M., and H.-U. Worm (2001), Anomalous unblocking temperatures, viscosity and frequency-dependency susceptibility in the chemically-remagnetized Trenton limestone, *Phys. Earth Planet. Inter.*, *126*, 27–42.
- Kukla, G., F. Heller, X. M. Liu, T. C. Xu, T. S. Liu, and Z. S. An (1988), Pleistocene climates in China dated by magnetic susceptibility, *Geology*, *16*, 811–814.
- Kukla, G., Z. S. An, J. L. Melice, J. Gavin, and J. L. Xiao (1990), Magnetic susceptibility record of Chinese loess, *Trans. R. Soc. Edinburgh Earth Sci.*, *81*, 263–288.
- Liu, Q. S. (2004), Pedogenesis and its effects on the natural remanent magnetization acquisition history of the Chinese loess, Ph.D. thesis, Univ. of Minn., Minneapolis.
- Liu, Q., M. J. Jackson, Y. Yu, F. Chen, C. Deng, and R. Zhu (2004a), Grain size distribution of pedogenic magnetic particles in Chinese loess/paleosols, *Geophys. Res. Lett.*, *31*, L22603, doi:10.1029/2004GL021090.
- Liu, Q., S. K. Banerjee, M. J. Jackson, B. A. Maher, Y. Pan, R. Zhu, C. Deng, and F. Chen (2004b), Grain sizes of susceptibility and anhysteretic remanent magnetization carriers in Chinese loess/paleosol sequences, *J. Geophys. Res.*, *109*, B03101, doi:10.1029/2003JB002747.
- Liu, Q. S., S. K. Banerjee, M. J. Jackson, F. H. Chen, Y. X. Pan, and R. X. Zhu (2004c), Determining the climatic boundary between the Chinese loess and paleosol: Evidence from aeolian coarse-grained magnetite, *Geophys. J. Int.*, *156*, 267–274.
- Maher, B. A. (1988), Magnetic properties of some synthetic sub-micron magnetites, *Geophys. J.*, *94*, 83–96.
- Maher, B. A. (1998), Magnetic properties of modern soils and Quaternary loessic paleosols: Paleoclimatic implications, *Palaeogeogr. Palaeoclimatol. Palaeoecol.*, *137*, 25–54.
- Maher, B. A., and R. Thompson (1991), Mineral magnetic record of the Chinese loess and paleosols, *Geology*, *19*, 3–6.
- Maher, B. A., and R. Thompson (1992), Paleoclimatic significance of the mineral magnetic record of the Chinese loess and paleosols, *Quat. Res.*, *37*, 155–170.
- Maher, B. A., and R. Thompson (1995), Paleorainfall reconstructions from pedogenic magnetic susceptibility variations in the Chinese loess and paleosols, *Quat. Res.*, *44*, 383–391.
- Maher, B. A., and R. Thompson (Eds.) (1999), *Quaternary Climates, Environments, and Magnetism*, Cambridge Univ. Press, New York.
- Maher, B. A., A. O. Alekseev, and T. Alekseeva (2003), Magnetic mineralogy of soils across the Russian steppe: Climate dependence of pedogenic magnetite formation, *Palaeogeogr. Palaeoclimatol. Palaeoecol.*, *201*, 321–341.
- Mishima, T., M. Torii, H. Fukusawa, Y. Ono, X. M. Fang, B. T. Pan, and J. J. Li (2001), Magnetic grain size distribution of the enhanced component in the loess paleosol sequences in the western Loess Plateau of China, *Geophys. J. Int.*, *145*, 499–504.
- Néel, L. (1949), Theorie du trainage magnétique des ferromagnétiques en grains fins avec application aux terres cuites, *Ann. Géophys.*, *5*, 99–136.
- Porter, S. C. (2001), Chinese loess record of monsoon climate during the last glacial-interglacial cycle, *Earth Sci. Rev.*, *54*, 115–128.
- Schwertmann, U. (1989), Occurrence and formation of iron oxides in the various paleoenvironments, in *Iron in Soils and Clay Minerals*, edited by J. W. Stucki, B. A. Goodman, and U. Schwertmann, pp. 267–308, Springer, New York.
- Sun, W. W., S. K. Banerjee, and C. P. Hunt (1995), The role of maghemite in the enhancement of magnetic signal in the Chinese loess-paleosol sequence: An extensive rock magnetic study combined with citrate-bicarbonate-dithionite treatment, *Earth Planet. Sci. Lett.*, *133*, 493–505.
- Tang, Y. J., J. Y. Jia, and X. D. Xie (2003), Records of magnetic properties in Quaternary loess and its paleoclimatic significance: A brief review, *Quat. Int.*, *108*, 33–50.
- Taylor, R. M., B. A. Maher, and P. G. Self (1987), Magnetite in soils I. The synthesis of single-domain and superparamagnetic magnetite, *Clays Clay Miner.*, *22*, 411–422.
- Thompson, R., and B. A. Maher (1995), Age models, sediment fluxes and palaeoclimatic reconstructions for the Chinese loess and paleosol sequences, *Geophys. J. Int.*, *123*, 611–622.
- Thompson, R., and F. Oldfield (1986), *Environmental Magnetism*, 227 pp., Allen and Unwin, St Leonards, N.S.W., Australia.
- van Velzen, A. J., and M. J. Dekkers (1999), The incorporation of thermal methods in mineral magnetism of loess-paleosol sequences: A brief overview, *Chin. Sci. Bull.*, *44*, 53–63.
- Verosub, K. L., P. Fine, M. J. Singer, and J. TenPas (1993), Pedogenesis and paleoclimate: Interpretation of the magnetic susceptibility record of Chinese loess-paleosol sequences, *Geology*, *21*, 1011–1014.
- Worm, H.-U. (1998), On the superparamagnetic-stable single domain transition for magnetite and frequency dependency of susceptibility, *Geophys. J. Int.*, *133*, 201–206.
- Yu, Y., D. J. Dunlop, and Ö. Özdemir (2002), Partial anhysteretic remanent magnetization in magnetite: 1. Additivity, *J. Geophys. Res.*, *107*(B10), 2244, doi:10.1029/2001JB001249.
- Yu, Y., L. Tauxe, and B. M. Moskowitz (2004), Temperature dependence of magnetic hysteresis, *Geochem. Geophys. Geosyst.*, *5*, Q06H11, doi:10.1029/2003GC000685.
- Zhou, L. P., F. Oldfield, A. G. Wintle, S. G. Robinson, and J. T. Wang (1990), Partly pedogenic origin of magnetic variations in Chinese loess, *Nature*, *346*, 737–739.

C. Deng and R. Zhu, Paleomagnetism and Geochronology Laboratory (SKL-LE), Institute of Geology and Geophysics, Chinese Academy of Sciences, Beijing 100029, China. (cldeng@mail.iggcas.ac.cn; rxzhu@mail.iggcas.ac.cn)

Q. Liu, Institute for Rock Magnetism, Department of Geology and Geophysics, University of Minnesota, 291 Shepherd Labs, 100 Union Street S.E., Minneapolis, MN 55455-0128, USA. (liu0272@yahoo.com)

B. A. Maher, Centre for Environmental Magnetism and Palaeomagnetism, Lancaster Environment Centre, Geography Department, Lancaster University, Lancaster LA1 4YW, UK. (b.maher@lancaster.ac.uk)

J. Torrent, Departamento de Ciencias y Recursos Agrícolas y Forestales, Universidad de Córdoba, Edificio C4, Campus de Rabanales, E-14071 Córdoba, Spain. (cr1tocaj@uco.es)

Y. Yu, Geosciences Research Division, Scripps Institution of Oceanography, 9500 Gilman Dr., La Jolla, CA 92093, USA. (yjyu@ucsd.edu)

X. Zhao, Department of Earth Sciences, University of California, Santa Cruz, CA, USA.